Original Research Paper

Process Physics: Emergent Unified Dynamical 3-Space, Quantum and Gravity: a Review

Reginald Thomas Cahill

School of Chemical and Physical Sciences, Flinders University, Adelaide 5001, Australia

Abstract: Experiments have repeatedly revealed the existence of a dynamical structured fractal 3-space, with a speed relative to the Earth of some 500 km sec^{-1} from a southerly direction. Experiments have ranged from optical light speed anisotropy interferometers to zener diode quantum detectors. This dynamical space has been missing from theories from the beginning of physics. This dynamical space generates a growing universe and gravity when included in a generalised Schrodinger equation and light bending when included in generalised Maxwell equations. Here we review ongoing attempts to construct a deeper theory of the dynamical space starting from a stochastic pattern generating model that appears to result in 3-dimensional geometrical elements, "gebits" and accompanying quantum behaviour. The essential concept is that reality is a process and geometrical models for space and time are inadequate.

Keywords: Process Physics, Dynamical 3-Space, Gravity, Gravitational Waves, Generalised Schrodinger Equation, Stochastic Neural Network.

Introduction

The phenomena of space and time are much richer and more complex than captured by the prevailing geometrical models, which originated with the earliest work by Galileo and Newton. These geometrical models capture only very limited macroscopic properties, namely Euclidean geometry in the case of "space" and the quantification of "time" in its geometrical modelling. In the 20th century the amalgamation of these two geometrical models into the one "space-time" model has resulted in deeper problems, namely the disagreement with numerous experiments, which, as one example, reveal the anisotropy of the speed of light, but which is excluded by the space-time model. To develop a deeper unified model for space, time and quantum matter, it is essential that these phenomena are not built into the theory from the very beginning: Rather they should be emergent. One approach is that of "Process Physics", (Cahill, 2005a), which bootstraps a unified treatment of reality from a stochastic self-accessing and self-limiting stochastic network. In that sense the patterns posses a semantic information meaning, namely that the dynamical system self-recognises and interacts with patterns in a manner determined by the structure of the patterns, rather the entities being specified by syntactical rules, as in present day physics, in which symbols and the rules of manipulation are specified outside of the

theory, i.e., "laws of physics' are imposed. In Process Physics the aim is to have self-generated phenomena that determine their own interaction behaviours. In doing so we discover that reality has somewhat the appearance of a neural network in which entities exist as sustaining network patterns, which we characterise as "semantic information", i.e., information that has a meaning internal to the system. Only at a higher level can we extract and summarise, in a limited manner, emergent rules of existence and interaction, in the style of conventional physics.

Stochastic Pattern Formation: Space

Here we describe a model for a self-referentially limited neuraltype network and then how such a network results in emergent geometry and quantum behaviour and which, increasingly, appears to be a unification of space and quantum phenomena. Process Physics is a semantic information system and is devoid of a priori objects and their laws and so it requires a subtle bootstrap mechanism to set it up. We use a stochastic neural network, Fig. 1, having the structure of real-number valued connections or relational information strengths B_{ij} (considered as forming a square matrix) between pairs of nodes or pseudo-objects i and j. In standard neural networks the network information resides in both link and node variables, with the semantic

Science Publications

information residing in attractors of the iterative network. Such systems are also not pure in that there is an assumed underlying and manifest a priori structure.

The nodes and their link variables will be revealed to be themselves sub-networks of informational relations. To avoid explicit self-connections $B_{ii} \neq 0$ which are a part of the subnetwork content of i, we use antisymmetry $B_{ij} = -B_{ji}$ to conveniently ensure that $B_{ii} = 0$, Fig. 1b.

At this stage we are using a syntactical system with symbols B_{ij} and, later, rules for the changes in the values of these variables. This system is the syntactical seed for the pure semantic system. Then to ensure that the nodes and links are not remnant a priori objects the system must generate strongly linked nodes (in the sense that the B_{ij} for these nodes are much larger than the B_{ij} values for non- or weakly-linked nodes) forming a fractal network; then self-consistently the start-up nodes and links may themselves be considered as mere names for sub-networks of relations. For a successful suppression the scheme must display Self-Organised Criticality (SOC) which acts as a filter for the start-up syntax. The designation 'pure' refers to the notion that all seeding syntax has been removed. SOC is the process where the emergent behaviour displays universal criticality in that the behaviour is independent of the particular start-up syntax; such a startup syntax then has no ontological significance.

To generate a fractal structure we must use a non-linear iterative system for the B_{ij} values. These iterations amount to the necessity to introduce a time-like process. Any system possessing a priori 'objects' can never be fundamental as the explanation of such objects must be outside the system. Hence in Process Physics the absence of intrinsic undefined objects is linked with the phenomena of time, involving as it does an ordering of 'states', the present moment effect and the distinction between past and present. Conversely in non-Process Physics the necessity for a priori objects is related to the use of the non-process geometrical model of time, with this modelling and its geometrical-time metarule being

an approximate emergent description from process-time. In this way Process Physics arrives at a new modelling of time, process time, which is much more complex than that introduced by Galileo, developed by Newton and reaching its so-called high point but deeply flawed Einstein spacetime geometrical model. Unlike these geometrical models process-time does model the Now effect. Process Physics also shows that time cannot be modelled by any other structure, other than a timelike process, here an iterative scheme. There is nothing like time available for its modelling. The near obsession of theoretical physicists with the geometrical modelling of time and its accompanying notion of analytical determinism, has done much to retard the development of physics.

The stochastic neural network so far has been realised with one particular scheme involving a stochastic non-linear matrix iteration, see (1). The matrix inversion B^{-1} then models self-referencing in that it requires, in principle, all elements of B to compute any one element of B^{-1}. As well there is the additive Self-Referential Noise (SRN) w_{ij} which limits the self-referential relational information but, significantly, also acts in such a way that the network is innovative in the sense of generating semantic information, that is relational information which is internally meaningful. The emergent behaviour is believed to be completely generic in that it is not suggested that reality is a computation, rather it appears that reality has the form of a self-referential orderdisorder information system. It is important to note that Process Physics is a non-reductionist modelling of reality; the basic iterator (1) is premised on the general assumption that reality is sufficiently complex that self-referencing occurs and that this has limitations. Equation 1 is then a minimal bootstrapping implementation of these notions. At higher emergent levels this self-referencing manifests itself as interactions between emergent patterns, but other novel effects may also arise.
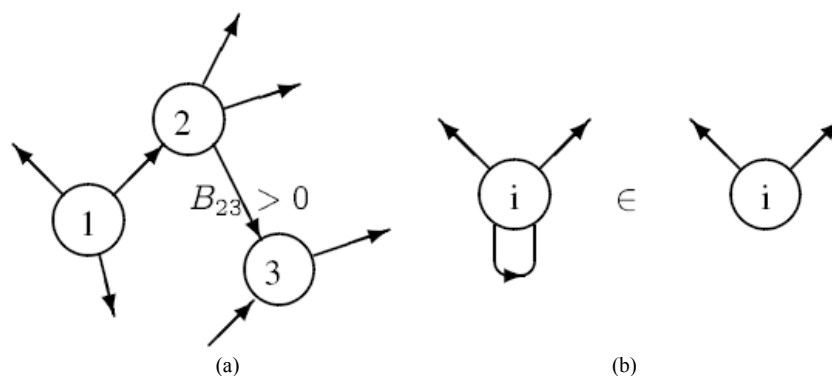

(a)   (b)

Fig. 1. (a) Graphical depiction of the neural network with links $B_{ij} \in R$ between nodes or pseudo-objects. Arrows indicate sign of B_{ij}. (b) Self-links are internal to a node, so $B_{ii} = 0$

To be a successful contender for the Theory Of Everything (TOE) Process Physics must ultimately prove the uniqueness conjecture: That the characteristics (but not the contingent details) of the pure semantic information system are unique.

This would involve demonstrating both the effectiveness of the SOC filter and the robustness of the emergent phenomenology and the complete agreement of the latter with observation.

The stochastic neural network is modelled by the iterative process Equation 1:

$$B_{ij} \rightarrow B_{ij} - a\left(B + B^{-1}\right)_{ij} + w_{ij}, i, j = 1, 2, ..., 2N \tag{1}$$

where, $w_{ij} = -w_{ji}$ are independent random variables for each ij pair and for each iteration and chosen from some probability distribution. Here at is a parameter the precise value of which should not be critical but which influences the self-organisational process.

Stochastic Networks from QFT

It may be helpful to outline the thoughts that led to (1), arising as it did from the quantum field theory frontier of quark physics. A highly effective approximation to Quantum Chromodynamics (QCD) was developed that made extensive use of bilocal fields and the Functional Integral Calculus (FIC), (Cahill, 1989; 1992; Cahill and Gunner 1998) for reviews of this Global Colour Model (GCM). In the GCM the bilocalfield correlators (giving meson and baryon correlators) are given by the generating functional:

$$Z[J] = \int DB^{\theta} \exp\left(-S[B] + \int d^4x d^4y B^{\theta}(x, y) J^{\theta}(x, y)\right) \tag{2}$$

Here $x, y \in E^4$, namely a Euclidean-metric space-time, as the hadronic correlators are required for vacuum-to-vacuum transitions and as is well known the use of the Euclidean metric picks out the vacuum state of the quantum field theory. The physical Minkowski-metric correlators are then obtained by analytic continuation $x_4 \rightarrow ix_0$. Equation 2 follows from (approximately) integrating out the gluon variables and then changing variables from the quark Grassmannian functional integrations to bilocal-field functional integrations. Here the θ index labels generators of flavour, colour and spin. This form is well suited to extracting hadronic phenomena as the vacuum state of QCD corresponds to a BCS-type superconducting state, with the $q\bar{q}$ Cooper pairs described by those non-zero mean-field $\bar{B}^{\theta}(x, y)$ determined by the Euler-Lagrange equations of the action Equation 3:

$$\frac{\delta S[B]}{\delta B^{\theta}(x, y)} = 0 \tag{3}$$

That (3) has non-zero solutions is the constituent-quark/BCSstate effect. This is a non-linear equation for those non-zero bilocal fields about which the induced effective action for hadronic fields is to be expanded.

Rather than approximately evaluating as a functional integral, as done in (Cahill, 1989; 1992; Cahill and Gunner 1998), we may use the Parisi-Wu stochastic 'quantisation' procedure (Parisi and Wu, 1981), which involves the Langevin iterative Equation 4:

$$B^{\theta}(x, y) \rightarrow B^{\theta}(x, y) - \frac{\delta S[B]}{\delta B^{\theta}(x, y)} + w^{\theta}(x, y) \tag{4}$$

where, $w^{\theta}(x, y)$ are Gaussian random variables with zero means. After many iterations a statistical equilibrium is achieved and the required hadronic correlators may be obtained by statistical averaging: $<B^{\theta}(x, y)B^{\phi}(u, v)... >$, but with again analytic continuation back to Minkowski metric required. In particular, writing:

$$B^{\theta}(x, y) = \phi\left(\frac{x+y}{2}\right)\Gamma\left(x - y, \frac{x+y}{2}\right)$$

Then $\phi(x)$ is a meson field, while $\Gamma(x, X)$ is the meson form factor.

That (4) leads to quantum behaviour is a remarkable result. The presence of the noise means that the full structure of $S[B]$ is explored during the iterations, whereas in (2) this is achieved by integration over all values of the $B^{\theta}(x, y)$ variables. The correlators $<B^{\theta}(x, y) B^{\phi}(u, v)... >$ correspond to complex quantum phenomena involving bound states of constituent quarks embedded in a BCS superconducting state. However the Euclidean-metric E^4-spacetime plays a completely classical and passive background role.

Now (4) has the form of a Stochastic Neural Network (SNN, see later), with link variables $B^{\theta}(x, y)$, that is, with the nodes being continuously distributed in E^4. An interesting question arises: If we strip away the passive classical E^4 background and the superscript indices, so that $B^{\theta}(x, y) \rightarrow B_{ij}$ and we retain only a simple form for $S[B]$, then does this discretised Langevin equation, in (1), which now even more so resembles a stochastic neural network, continue to display quantum behaviour? It has been found that indeed the SNN in (1) does exhibit quantum behaviour, by generating a quantum-foam dynamics for an emergent space and with quantum-'matter' being topological-defects embedded in that quantum-foam in a unification of quantum space and matter. Indeed the remarkable discovery is that (1) generates a quantum gravity. Note, however, that now the iterations in (1) correspond to physical time and we do not wait for equilibrium behaviour. Indeed the non-equilibrium behaviour manifests as a growing universe.

The iterations correspond to a non-geometric modelling of time with an intrinsic arrow of time, as the iterations in (1) cannot be reversed. Hence the description of this new physics as process physics.

If (1) does in fact lead to a unification of gravity and quantum theory, then the deep question is how should we interpret (1)? The stochastic noise has in fact been interpreted as the new intrinsic Self-Referential Noise when the connection with the work of Godel and Chaitin became apparent (Cahill, 2005a). Hence beneath quantum field theory there is evidence of a self-referential stochastic neural network and its interpretation as a semantic information system. Only by discarding the spacetime background of Quantum Field Theory (QFT) do we discover the necessity for space and the quantum.

Stochastic Neural Networks

We now briefly compare the iteration system in (1) to an Attractor Neural Network (ANN) and illustrate its basic mode of operation. An ANN has link $J_{ij} \in R$ and node $s_i = \pm 1$ variables ($i, j = 1, 2, \ldots N$), with $J_{ij} = J_{ji}$ and $J_{ii} = 0$. Here $s = +1$ denotes an active node, while $s = -1$ denotes an inactive node. The time evolution of the nodes is given by, for example Equation 5:

$$s_i(t) = \sin\left(\sum_j J_{ij} s_j(t-1)\right) \tag{5}$$

To imprint a pattern its $s_i \propto \xi_i$ values are imposed on the nodes and the Hebbian Rule is used to change the link strengths Equation 6:

$$J_{ij}(t) = J_{ij}(t-1) + c s_i(t-1) s_j(t-1) \tag{6}$$

And for p successively stored patterns ($\xi^1, \xi^2, \ldots \xi^p$) we end up with Equation 7:

$$J_{ij} = \sum_{\mu=1}^{p} \xi_i^\mu \xi_j^\mu, \quad i \neq j \tag{7}$$

The imprinted patterns correspond to local minima of the 'energy' function Equation 8:

$$E[\{s\}] = -\frac{1}{2} \sum J_{ij} s_i s_j \tag{8}$$

Which has basins of attraction when the ANN is 'exposed' to an external input $s_i(0)$. As is well known over iterations of (5) the ANN node variables converges to one of the stored patterns most resembling $s_i(0)$. Hence the network categorises the external input.

The iterator (1), however, has no external inputs and its operation is determined by the detailed interplay between the order/disorder terms. As well it has no node variables: Whether a node i is active is determined implicitly by $|B_{ij}| > b$, for some, where b is some minimum value for the link variables.

Because B_{ij} is antisymmetric and real its eigenvalues occur in pairs: ib, $-ib$ (b real), with a complete set of orthonormal eigenvectors ξ^μ, $\mu = \pm 1$, $\pm 2, \ldots, \pm N$, ($\xi^{\mu*} = \xi^{-\mu}$) so that Equation 9:

$$B_{jk} = \sum_{\mu=\pm 1, \pm 2, \ldots} ib_\mu \xi_j^\mu \xi_k^{\mu*}, b_\mu = -b_{-\mu} \in R \tag{9}$$

where, the coefficients must occur in conjugate pairs for real B_{ij}. This corresponds to the form Equation 10:

$$B = MDM^{-1}, D = \begin{pmatrix} 0 & +b_1 & 0 & 0 & \\ -b_1 & 0 & 0 & 0 & \\ 0 & 0 & 0 & +b_2 & \\ 0 & 0 & -b_2 & 0 & \\ & & & & \cdot \\ & & & & & \cdot \end{pmatrix} \tag{10}$$

where, M is a real orthogonal matrix. Both the b_μ and M change with each iteration.

Let us consider, in a very unrealistic situation, how patterns can be imprinted unchanged into the SNN. This will only occur if we drop the B^{-1} term in (1). Suppose the SRN is frozen (artificially) at the same form on iteration after iteration. Then iterations of (1) converge to Equation 11:

$$B = \frac{1}{a}w = \sum_\mu ia^{-1}w_\mu \eta_j^\mu \eta_k^{\mu*} \tag{11}$$

where w^μ and η^μ are the eigensystem for w. This is analogous to the Hebbian rule (6) and demonstrates the imprinting of w, which is strong for small a. If that 'noise' is now 'turned-off' then this imprinted pattern will decay, but do so slowly if a is small. Hence to maintain an unchanging imprinted pattern it needs to be continually refreshed via a fixed w. However the iterator with the B^{-1} term present has a significantly different and richer mode of behaviour as the system will now generate novel patterns, rather than simply imprinting whatever pattern is present in w. Indeed the system uses special patterns (the gebits) implicit in a random w that are used as a resource with which much more complex patterns are formed.

The task is to determine the nature of the self-generated patterns and to extract some effective descriptive syntax for that behaviour, remembering that the behaviour is expected to be quantum-like.

Emergent Geometry in Stochastic Networks: Gebits

We start the iterations of (1) at $B \approx 0$, representing the absence of information, that is, of patterns. With the noise absent the iterator behaves in a deterministic and reversible manner giving a condensate-like system with a B matrix of the form in (10) or (12), but with the matrix M iteration independent and determined uniquely by the start-up B and each b_μ evolves according to the iterator $b_\mu \to b_\mu - a(b_\mu - b_\mu^{-1})$, which converges to $b_\mu = \pm 1$. The corresponding eigenvectors ξ^μ do not correspond to any meaningful patterns as they are determined entirely by the random values from the startup $B \approx 0$. However in the presence of the noise the iterator process is non-reversible and non-deterministic and, most importantly, non-trivial in its pattern generation. The iterator is manifestly non-geometric and non-quantum in its structure and so does not assume any of the standard features of syntax based non-Process Physics models. Nevertheless, as we shall see, it generates geometric and quantum behaviour. The dominant mode is the formation of an apparently randomised background (in B) but, however, it also manifests a self-organising process which results in non-trivial patterns which have the form of a growing three-dimensional fractal process-space displaying quantum-foam behaviour. These patterns compete with this random background and represent the formation of a 'universe'.

The emergence of order in this system might appear to violate expectations regarding the 2nd Law of Thermodynamics; however because of the SRN the system behaves as an open system and the growth of order arises from the self referencing term, B^{-1} in (1), selecting certain implicit order in the SRN. Hence the SRN acts as a source of negentropy the term negentropy was introduced by Schrodinger (1944) and since then there has been ongoing discussion of its meaning. In Process Physics it manifests as the SRN.

This growing three-dimensional fractal process-space is an example of a Prigogine far-from-equilibrium dissipative structure driven by the SRN (Nicholis and Prigogine, 1997). From each iteration the noise term will additively introduce rare large value w_{ij}. These w_{ij}, which define sets of strongly linked nodes, will persist through more iterations than smaller valued w_{ij} and, as well, they become further linked by the iterator to form a three-dimensional process-space with embedded topological defects. In this way the stochastic neural network creates stable strange attractors and as well determines their interaction properties. This information is all internal to the system; it is the semantic information within the network.

We introduce, for convenience only, some terminology: We think of B_{ij} as indicating the connectivity or relational strength between two monads i and j. The monads concept was introduced by Leibniz, who espoused the relational mode of thinking in response to and in contrast with Newton's absolute space however we see later that these two concepts are indeed compatible, but only by enlarging the meaning of 'absolute space' Equation 12 and 13:

$$B_c = \begin{pmatrix} 0 & +1 & 0 & 0 & \\ -1 & 0 & 0 & 0 & \\ 0 & 0 & 0 & +1 & \\ 0 & 0 & -1 & 0 & \\ & & & & \ddots \end{pmatrix} \qquad (12)$$

$$B = \begin{pmatrix} g_1 & & & & \\ & \bigcirc & & & \\ & & g_2 & & \\ & & & g_3 & \\ & & & & c_1 & \\ & & & & & c_2 \end{pmatrix} \qquad (13)$$

The monad i has a pattern of dominant (larger valued B_{ij}) connections $B_{i1}, B_{i2}, ...,$ where $B_{ij} = -B_{ji}$ avoids self-connection ($B_{ii} = 0$) and real number valued. The self-referential noise $w_{ij} = -w_{ji}$ are independent random variables for each ij and for each iteration and with variance η. With the noise absent the iterator converges to one of the condensate $MB_c M^{-1}$ where the matrix M depends on the initial B. This behaviour is similar to the condensate of Cooper pairs in QFT, but here the condensate (indicating a non-zero dominant configuration) does not have any space-like structure. However in the presence of the noise, after an initial chaotic behaviour when starting the iterator from $B \approx 0$, the dominant mode is the formation of a randomised condensate $C \approx \mu \otimes B_c + B_b$, up to an orthogonality transformation, indicating B_c but with the ± 1's replaced by $\pm\mu_i$'s (where the μ_i are small and given by a computable iteration-dependent probability distribution $M(\mu)$) and with a noisy background B_b of very small B_{ij}.

The key discovery is that there is an extremely small self-organising process buried within this condensate and which has the form of a three-dimensional fractal process-space, which we now explain. Consider the connectivity from the point of view of one monad, call it monad i. Monad i is connected via these large B_{ij} to a number of other monads and the whole set of connected monads forms a tree-graph relationship. This is because the large links are very improbable and a tree-graph relationship is much more probable than a similar graph involving the same monads but with additional links. The set of all large valued B_{ij} then form treegraphs

disconnected from one-another; Fig. 2. In any one tree-graph the natural 'distance' measure for any two monads within a graph is the smallest number of links connecting them. Let $D_1, D_2, ..., D_L$ be the number of nodes of distance 1, 2, ..., L from monad i (define $D_0 = 1$ for convenience), where L is the largest distance from i in a particular tree-graph and let N be the total number of nodes in the tree. Then $\sum_{k=0}^{L} D_k = N$; Fig. 2 for an example.

Now consider the number $N(D,N)$ of different random N-node trees, with the same distance distribution $\{D_k\}$, to which i can belong. By counting the different linkage patterns, together with permutations of the monads we obtain Equation 14:

$$N(D,N) = \frac{(M-1)! D_1^{D_2} D_2^{D_3} ... D_{L-1}^{D_L}}{(M-N-2)! D_1! D_2! ... D_L!} \quad (14)$$

Here $D_k^{D_k+1}$ is the number of different possible linkage patterns between level k and level $k+1$ and $(M-1)!/(M-N-2)!$ Is the number of different possible choices for the monads, with i fixed. The denominator accounts for those permutations which have already been accounted for by the $D_k^{D_k+1}$ factors. We compute the most likely tree-graph structure by maximising $\ln N(D,N) + \lambda \left(\sum_{k=0}^{L} D_k - N \right)$ where λ is a Lagrange multiplier for the constraint. Using Stirling's approximation for $D_k!$ we obtain:

$$D_{k+1} = D_k \ln \frac{D_k}{D_{k-1}} - \lambda D_k + \frac{1}{2} \quad (15)$$

We may compute the most likely tree-graph structure by maximising $N(D,N)$ with respect to $\{D_k\}$. This equation has an approximate analytic solution (Nagels, 1985):

$$D_k = \frac{2N}{L} \sin^2 (\pi k / L)$$

These results imply that the most likely tree-graph structure to which a monad can belong has a distance distribution $\{D_k\}$ which indicates that the tree-graph is embeddable in a 3-dimensional hypersphere, S^3.

We call these tree-graph B-sets gebits (geometrical bits). However S^3 embeddability of these gebits is a weaker result than demonstrating the necessary emergence of S^3-spaces, since extra cross-linking connections would be required for this to produce a strong embed ability.

The monads for which the B_{ij} are, from the SRN term, large thus form disconnected gebits and in (13) we relabel the monads to bring these new gebits $g_1, g_2, g_3, ..$

to block diagonal form, with the remainder indicating the small and growing thermalised condensate, $C = c_1 \oplus c_2 \oplus c_3 ...$ In (13) the g_i indicate unconnected gebits, while the icon $\bigcirc$ represents older and connected gebits and suggests a compact 3-space. The remaining very small B_{mn}, not shown in (13), are background noise only.

A key dynamical feature is that most gebit matrices g have $\det(g) = 0$, since most tree-graph connectivity matrices are degenerate. For example in the tree in Fig. 2 the B matrix has a nullspace, spanned by eigenvectors with eigenvalue zero, of dimension two irrespective of the actual values of the non-zero B_{ij}; for instance the right hand pair ending at the level $D_2 = 4$ are identically connected and this causes two rows (and columns) to be identical up to a multiplicative factor. So the degeneracy of the gebit matrix is entirely structural. For this graph there is also a second set of three monads whose connectivities are linearly dependent. These $\det(g) = 0$ gebits form a reactive gebits subclass, i.e. in the presence of background noise $(g_1 \oplus g_2 \oplus g_3 \oplus ..)^{-1}$ is well-defined and has some large elements. These reactive gebits are the building blocks of the dissipative structure. The self-assembly process is as follows: Before the formation of the thermalised condensate B^{-1} generates new connections (large B_{ij}) almost exclusively between gebits and the remaining non-gebit sub-block (having $\det \approx 0$ but because here all the involved $B_{ij} \approx 0$), resulting in the decay, without gebit interconnection, of each gebit. However once the condensate has formed (essentially once the system has 'cooled' sufficiently) the condensate $C = c_1 \oplus c_2 \oplus c_3 \oplus ...$ acts as a quasi-stable (i.e., $\det(C) = \Pi_i \det(c_i) \neq 0$) sub-block of (13) and the sub-block of gebits may be inverted separately. The gebits are then interconnected (with many gebits present cross-links are more probable than self-links) via new links formed by B^{-1}, resulting in the larger structure indicated by the $\bigcirc$ in (13). Essentially, in the presence of the condensate, the gebits are sticky.

Now (14) is strictly valid in the limit of vanishingly small probabilities. For a more general analysis of the connectivity of such gebits assume for simplicity that the large w_{ij} arise with fixed but very small probability p, then the emergent geometry of the gebits is revealed by studying the probability distribution for the structure of the random graph units or gebits minimal spanning trees with D_k nodes at k links from node i ($D_0 \equiv 1$), this is given more generally in the next section.

Gebit Connectivity

The probability that a connected random graph with N vertices has a depth structure $D_0, D_1, ..., D_L$ is given in (22) and leads to the concept of emergent geometry via the gebit concept. Equation 22 was first derived by Nagels (1985).
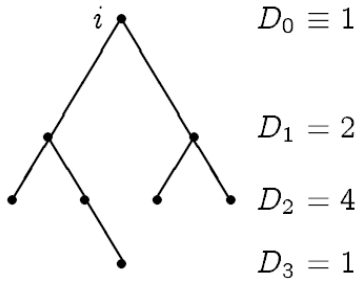
Fig. 2. An $N = 8$ spanning tree for a random graph (not shown) with $L = 3$. The distance distribution D_k is indicated for node i

Consider a set of M nodes with pairwise links arising with probability $p \ll 1$. The probability of nonlinking is then $q = 1\text{-}p$. We shall term linked nodes as being 'adjacent', though the use of this geometric language is to be justified and its limitations determined. The set M will be partitioned into finite subsets of mutually disconnected components, each having N_i nodes which are at least simply connected-that is, each N_i may be described by a non-directed graph.

Consider one of these components, with $N = N_i \gg 1$ and choose one vertex to be the 'origin'. We will determine the probable distribution of vertices in this component as measured by the depth structure of a minimal spanning tree. Figure 2 for the definition of depth structure. Let D_k be the number of vertices at a distance k from the origin then $D_0 = 1$ is the origin, D_1 is the number of adjacent vertices or nearest neighbours to the origin and D_2 is the number of next nearest neighbours and so on. Then, since N is finite, there is a maximum distance L on the graph and D_L is the number of vertices at this maximum distance from the origin. There is then the constraint Equation 16 and 17:

$$\sum_{k=0}^{L} D_k = N \tag{16}$$

And also:

$$\begin{cases} D_0 = 1 \\ D_k > 0, \quad 0 \le k \le L, \\ D_k = 0, \quad k > L \end{cases} \tag{17}$$

To calculate the probability for the distribution:

$$\left\{ D_k : 0 \le k \le N, \sum_{k=0}^{N-1} D_k = N \right\}$$

We require:

The probability for the number D_1 of nearest neighbours (i.e., those vertices at unit distance from the origin) is p^{D_1}, which may be written as $(1-q)^{D_1} = \left(1-q_0^{D_0}\right)^{D_1}$, since $D_0 = 1$

The probability for the next nearest neighbours, D_2, is obtained by considering that any vertex at this level is:

- Adjacent to at least one point at unit distance from the origin
- Not adjacent to the origin itself

Condition (b) is easily obtained since it occurs with probability $q = 1\text{-}p$ so there is a factor of q^{D_2} for this.

Condition (a) may be obtained by first considering the counter argument i.e., that the vertex is not adjacent to any of the D_1. This has probability q^{D_1}. Thus the probability that it is adjacent to at least one of the D_1 is just $1-q^{D_1}$. So there is an overall factor of $\left(1-q^{D_1}\right)^{D_2}$ for this condition.

Hence, the probability of obtaining D_2 is the product of these two factors i.e., Equation 18:

$$prob\left(D_2\right) = \left(1-q^{D_1}\right)^{D_2} q^{D_2} \tag{18}$$

The probability for D_3, those vertices at distance $k = 3$ from the origin, is similarly defined by the requirements that a vertex in D_3 is:

- Adjacent to least one vertex in D_2
- Not adjacent to any vertex in D_1
- Not adjacent to the origin

Condition (a) is argued precisely as the corresponding condition in item 2 above, i.e., it provides a factor $\left(1-q^{D_2}\right)^{D_3}$.

Condition (b) is expressed as q^{D_1}, thus providing the factor $\left(q^{D_1}\right)^{D_3}$.

Conditioned (c) is satisfied simply by the factor q^{D_3}, which may be written as $\left(q^{D_0}\right)^{D_3}$ since $D_0 \equiv 1$. Hence the probability of obtaining D_3 is Equation 19:

$$\left(1-q^{D_2}\right)^{D_3} \left(q^{D_1}\right)^{D_3} \left(q^{D_0}\right)^{D_3} = \left(q^{D_0+D_1}\right)^{D_3} \left(1-q^{D_2}\right)^{D_3} \tag{19}$$

For vertices at a distance $i+1$ from the origin, induction on the previous results gives Equation 20:

$$prob\left(D_{i+1}\right) = \left(q^{\sum_{j=0}^{i-1} D_j}\right)^{D_{i+1}} \left(1-q^{D_i}\right)^{D_{i+1}} \tag{20}$$

So the probability P for the depth distribution is the probability of obtaining a particular set $(D_1, \cdots, D_L)$ which is Equation 21:

$$P = p^{D_1} \prod_{i=1}^{L-1} \left(q \sum_{j=0}^{i-1} D_j \right)^{D_{i+1}} \left(1 - q^{D_i} \right)^{D_{i+1}} \qquad (21)$$

Note that vertices may be permuted between the sets of vertices at different distances. That is, the same magnitudes for each D_k could be obtained by many other possible configurations which result from a relabelling of the graph. First, there are $(N\text{-}1)!$ ways of relabelling the graph once the choice of origin has been fixed so there are $(N\text{-}1)!$ Ways of obtaining the same P, where the depth structure given by $(D_1, D_2, \cdots, D_L)$ is identical. Second, the number of instances of a particular shape irrespective of labelling (beyond the choice of origin) is given by the product $D_1! D_2! \cdots D_L!$.

Hence there are $\dfrac{(N-1)!}{D_1! D_2! \cdots D_L!}$ ways of obtaining a graph (from a fixed origin) with a particular depth structure and therefore, the probability for a specified shape with N given and the origin arbitrarily chosen, that is, the probability distribution, is:

$$P = \frac{(N-1)!}{D_1! D_2! ... D_L!} p^{D_1} \prod_{i=1}^{L-1} \left(q \sum_{j=0}^{i-1} D_j \right)^{D_{i+1}} \cdot \left(1 - q^{D_i} \right)^{D_{i+1}} \qquad (22)$$

where $q = 1\text{-}p$, N is the total number of nodes in the gebit and L is the maximum depth from node i. In the limit $p \to 0$ (22) reduces to (14), proportionally. To find the most likely connection pattern we numerically maximise $P[D, L, N]$ for fixed N with respect to L and the D_k. The resulting L and $\{D_1, D_2, ..., D_L\}$ fit very closely to the form:

$$D_k \propto \sin^{d-1}\left(\pi k / L \right)$$

Figure 3a, for $N = 5000$ and $\mathrm{Log}_{10} p = -6$. The resultant d values for a range of $\mathrm{Log}_{10} p$ and with $N = 5000$ are shown in Fig. 3b.

This shows, for p below a critical value, that $d = 3$, indicating that the connected nodes have a natural embedding in a 3D hypersphere S^3, call this a base gebit. Above that value of p, the increasing value of d indicates the presence of extra links that, while some conform with the embeddability, others are in the main defects with respect to the geometry of the S^3. These extra links act as topological defects. By themselves these extra links will have the connectivity and embedding geometry of numbers of gebits, but these gebits have a 'fuzzy' embedding in the base gebit. This is an indication of fuzzy homotopies (a homotopy is, put simply, an embedding of one space into another). Here we see the emergence of geometry, not only of space but also of the internal flavour symmetry spaces of quantum fields. The nature of the resulting 3D process-space is suggestively indicated in Fig. 3c and behaves essentially as a quantum foam.
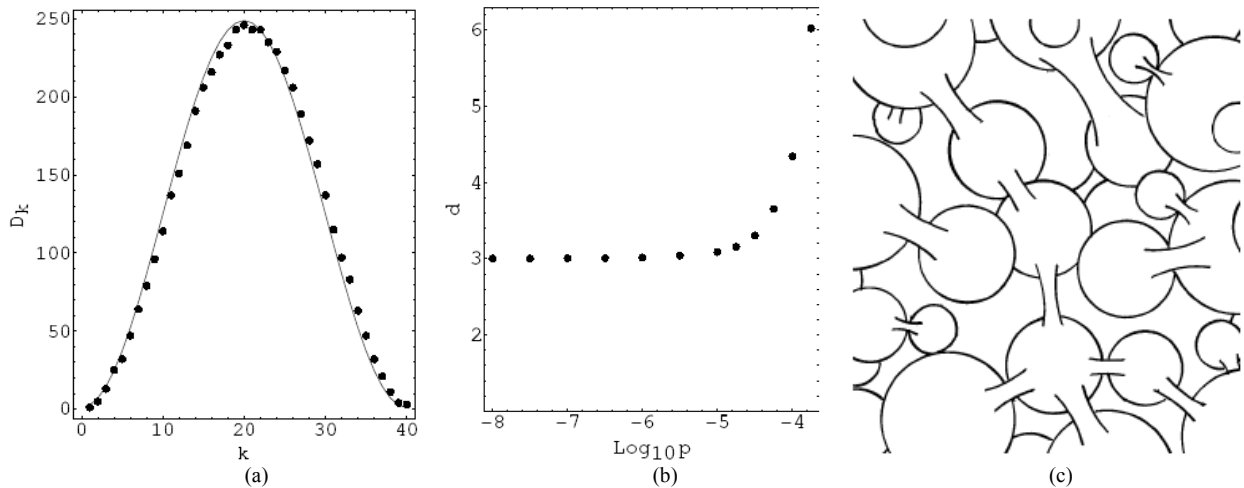

Fig. 3. Top: Points show the D_k set and $L = 40$ value found by numerically maximising $P[D, L, N]$ for $\mathrm{Log}_{10} p = -6$ for fixed $N = 5000$. Curve shows $D_k \propto \sin^{d-1}\left(\dfrac{\pi k}{L} \right)$ with best fit $d = 3.16$ and $L = 40$, showing excellent agreement and indicating embeddability in an S^3 with some topological defects. Middle: Dimen d of the gebits as a function of the probability p. Bottom: Graphical depiction of the 'process space' at one stage of the iterative process-time showing a quantum-foam structure formed from embeddings and links. The linkage connections have the distribution of a 3D space, but the individual gebit components are closed compact spaces and cannot be embedded in a 3D background space. So the drawing is only suggestive. Nevertheless this figure indicates that Process Physics generates a cellular information system, where the behaviour is determined at all levels by internal information

Over ongoing iterations the existing gebits become crosslinked and eventually lose their ability to undergo further linking; they lose their 'stickiness' and decay. The value of the parameter a in (1) must be small enough that the 'stickiness' persists over many iterations, that is, it is not quenched too quickly, otherwise the emergent network will not grow. Hence the emergent space is 3D but is continually undergoing replacement of its component gebits; it is an informational process-space, in sharp distinction to the non-process continuum geometrical spaces that have played a dominant role in modelling physical space. If the noise is 'turned off' then this emergent dissipative space will decay and cease to exist. We thus see that the nature of space is deeply related to, as implemented here, a self-referentially limited neural network.

Gebits as Skyrmions

We need to extract convenient but approximate syntactical descriptions of the semantic information in the network and these will have the form of a sequence of mathematical constructions, the first being the Quantum Homotopic Field Theory. Importantly they must all retain explicit manifestations of the SRN. To this end first consider the special case of the iterator when the SRN is frozen at a particular w, that is we consider iterations with an artificially fixed SRN term. Then it may be shown that the iterator is equivalent to the minimisation of an 'energy' expression (remember that B and w are antisymmetric) Equation 23:

$$E[B;w] = -\frac{a}{2}Tr[B^2] - aTrLn[B] + Tr[wB] \qquad (23)$$

Note that for disconnected gebits g_1 and g_2 this energy is additive, $E[g_1 \oplus g_2] = E[g_1] + E[g_2]$. Now suppose the fixed w has the form of a gebit approximating an S^3 network with one embedded topological defect which is itself an S^3 network, for simplicity. So we are dissecting the gebit into base gebit, defect gebit and linkings or embeddings between the two. We also ignore the rest of the network, which is permissible if our gebit is disconnected from it. Now if $\det(w)$ is not small, then this gebit is non-sticky and for small a, the iterator converges to $B \approx \frac{1}{a}w$, namely an enhancement only of the gebit. However because the gebits are rare constructs they tend to be composed of larger w_{ij} forming tree structures, linked by smaller valued w_{ij}. The tree components make $\det(w)$ smaller and then the inverse B^{-1} is activated and generates new links. Hence, in particular, the topological defect

relaxes, according to the 'energy' measure, with respect to the base gebit. This relaxation is an example of a 'non-linear elastic' process (Ogden, 1984). The above gebit has the form of a mapping $\pi: S \rightarrow \Sigma$ from a base space to a target space. Manton and Ruback (1985; Manton, 1987) has constructed the continuum form for the 'elastic energy' of such an embedding and for $\pi: S^3 \rightarrow S^3$ it is the Skyrme energy Equation 24:

$$E[U] = \int \left[\begin{array}{c} -\frac{1}{2}Tr\left(\partial_i UU^{-1}\partial_i UU^{-1}\right) \\ -\frac{1}{16}Tr\left[\partial_i UU^{-1}, \partial_i UU^{-1}\right]^2 \end{array} \right] \qquad (24)$$

where, $U(x)$ is an element of $SU(2)$. Via the parametrisation $U(x) = \sigma(x) + i\vec{\pi}(x).\vec{\tau}$, where the τ_i are Pauli matrices, we have $\sigma(x)^2 + \vec{\pi}(x)^2 = 1$, which parametrises an S^3 as a unit hypersphere embedded in E^4 (which has no ontological significance, of course). Non-trivial minima of $E[U]$ are known as Skyrmions (a form of topological soliton) and have $Z = \pm1, \pm2, \ldots$, where Z is the winding number of the map Equation 25:

$$Z = \frac{1}{24\pi^2}\int\sum \epsilon_{ijk}Tr\left(\partial_i UU^{-1}\partial_j UU^{-1}\partial_k UU^{-1}\right) \qquad (25)$$

The first key to extracting emergent phenomena from the stochastic neural network is the validity of this continuum analogue, namely that $E[B;w]$ and $E[U]$ are describing essentially the same 'energy' reduction process. This requires detailed analysis.

Absence of a Cosmic Code

This 'frozen' SRN analysis of course does not match the time-evolution of the full iterator (1), for this displays a much richer collection of processes. With ongoing new noise in each iteration and the saturation of the linkage possibilities of the gebits emerging from this noise, there arises a process of ongoing birth, linking and then decay of most patterns. The task is then to identify those particular patterns that survive this flux, even though all components of these patterns eventually disappear and to attempt a description of their modes of behaviour. This brings out the very biological nature of the information processing in the SNN and which appears to be characteristic of a 'pure' semantic information system. Kitto (2002) has further investigated the analogies between Process Physics and living systems. The emergent 'laws of physics' are the habitual habits of this system and it appears that they may be identified. However there is no encoding

mechanism for these 'laws', they are continually manifested; there is no cosmic code. In contrast living or biological systems could be defined as those emergent patterns which discovered how to encode their 'laws' in a syntactical genetic code. Nevertheless such biological systems make extensive use of semantic information at all levels as their genetic code is expressed in the phenotype.

Entrapped Topological Defects

In general each gebit, as it emerges from the SRN, has active nodes and embedded topological defects, again with active nodes. Further there will be defects embedded in the defects and so on and so gebits begin to have the appearance of a fractal defect structure and with all the defects having various classifications and associated winding numbers. The energy analogy above suggests that defects with opposite winding numbers at the same fractal depth may annihilate by drifting together and merging. Furthermore the embedding of the defects is unlikely to be 'classical', in the sense of being described by a mapping $\pi(x)$, but rather would be fuzzy, i.e., described by some functional, $F[\pi]$, which would correspond to a classical embedding only if F has a very sharp supremum at one particular $\pi = \pi_{cl}$. As well these gebits are undergoing linking because their active nodes (Cahill and Klinger, 2000) activate the B^{-1} new-links process between them and so by analogy the gebits themselves form larger structures with embedded fuzzy topological defects. This emergent behaviour is suggestive of a quantum space foam, but one containing topological defects which will be preserved by the system, unless annihilation events occur. If these topological defects are sufficiently rich in fractal structure so as to be preserved, then their initial formation would have occurred as the process-space relaxed out of its initial essentially random form. This phase would correspond to the early stages of the Big-Bang. Once the topological defects are trapped in the process-space they are doomed to meander through that space by essentially self-replicating, i.e. continually having their components die away and be replaced by similar components. These residual topological defects are what we call matter. The behaviour of both the process-space and its defects is clearly determined by the same network processes; we have an essential unification of space and matter phenomena. This emergent quantum foam-like behaviour suggests that the full generic description of the network behaviour is via the Quantum Homotopic Field Theory (QHFT). We also see that cellular structures are a general feature of semantic information systems, with the information necessarily distributed.

Functional Schrodinger Equation

Because of the iterator the resource is the large valued B_{ij} from the SRN because they form the 'sticky' gebits which are self-assembled into the non-flat compact 3D process-space. The accompanying topological defects within these gebits and also the topological defects within the process space require a more subtle description. The key behavioural mode for those defects which are sufficiently large (with respect to the number of component gebits) is that their existence, as identified by their topological properties, will survive the ongoing process of mutation, decay and regeneration; they are topologically self-replicating. Consider the analogy of a closed loop of string containing a knot-if, as the string ages, we replace small sections of the string by new pieces then eventually all of the string will be replaced, however the relational information represented by the knot will remain unaffected as only the topology of the knot is preserved. In the process-space there will be gebits embedded in gebits and so forth, in topologically non-trivial ways; the topology of these embeddings is all that will be self-replicated in the processing of the dissipative structure.

To analyse and model the 'life' of these topological defects we need to characterise their general behaviour: If sufficiently large (i) they will self-replicate if topological nontrivial, (ii) we may apply continuum homotopy theory to tells us which embeddings are topologically non-trivial, (iii) defects will only dissipate if embeddings of 'opposite winding number' (these classify the topology of the embedding) engage one another, (iv) the embeddings will be in general fractal and (iv) the embeddings need not be 'classical', i.e., the embeddings will be fuzzy. To track the coarse-grained behaviour of such a system led to the development of a new form of quantum field theory: Quantum Homotopic Field Theory (QHFT). This models both the process-space and the topological defects.

To construct this QHFT we introduce an appropriate configuration space, namely all the possible homotopic mappings $\pi_{\alpha\beta}: S_\beta \rightarrow S_\alpha$, where the S_1, S_2, .., describing 'clean' or topological-defect free gebits, are compact spaces of various types. Then QHFT has the form of an iterative functional Schrodinger equation for the discrete time-evolution of a wave-functional $\Psi[...., \pi_{\alpha\beta}, ...;t]$:

$$\Psi\left[...., \pi_{\alpha\beta},....;t + \Delta t\right] = \Psi\left[...., \pi_{\alpha\beta},....;t\right] - iH\Psi\left[...., \pi_{\alpha\beta},....;t\right]\Delta t + QSD\ terms \tag{26}$$

This form arises as it is models the preservation of semantic information, by means of a unitary time

evolution; even in the presence of the noise in the Quantum State Diffusion (QSD, Percival, 1998) terms. Because of the QSD noise (26) is an irreversible quantum system. The time step Δt in (26) is relative to the scale of the fractal processes being explicitly described, as we are using a configuration space of mappings between prescribed gebits. At smaller scales we would need a smaller value for Δt. Clearly this invokes a (finite) renormalisation scheme. We now discuss the form of the hamiltonian and the QSD terms.

First (26), without the QSD term, has a form analogous to a 'third quantised' system, in conventional terminology (Coleman *et al.*, 1981). These systems were considered as perhaps capable of generating a quantum theory of gravity. The argument here is that this is the emergent behaviour of the SNN and it does indeed lead to quantum gravity, but with quantum matter as well. More importantly we understand the origin of (26) and it will lead to quantum and then classical gravity, rather than arise from classical gravity via some ad hoc or heuristic quantisation procedure.

Depending on the 'peaks' of Ψ and the connectivity of the resultant dominant mappings such mappings are to be interpreted as either embeddings or links; Fig. 4 then suggests the dominant process-space form within Ψ showing both links and embeddings. The emergent process-space then has the characteristics of a quantum foam. Note that, as indicated in Fig. 4, the original start-up links and nodes are now absent. Contrary to the suggestion in Fig. 4, this process space cannot be embedded in a finite dimensional geometric space with the emergent metric preserved, as it is composed of nested finitedimensional closed spaces.
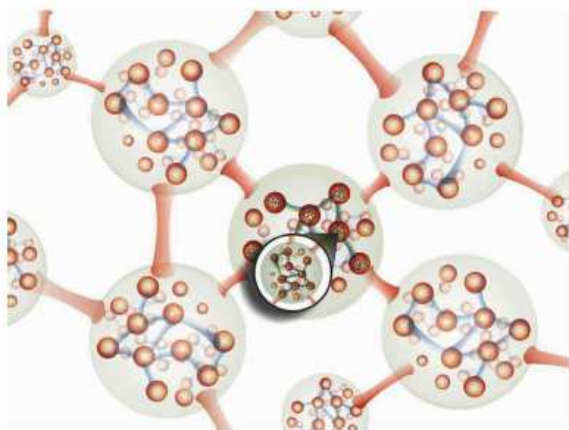

Fig. 4. An representation of the functional Ψ [{π}; *t*] showing dominant homotopies. The 'magnifying glass' indicates that these mappings can be nested, i.e., fractal

Homotopy Hamiltonian

We now consider the form of the hamiltonian H. In the previous sections it was suggested that Manton's non-linear elasticity interpretation of the Skyrme energy is appropriate to the SNN. This then suggests that H is the functional operator:

$$H = \sum_{\alpha \neq \beta} h\left[\frac{\delta}{\delta \pi_{\alpha\beta}}, \pi_{\alpha\beta}\right] \tag{27}$$

where, $h\left[\frac{\delta}{\delta\pi}, \pi\right]$ is the (quantum) Skyrme Hamiltonian functional operator for the system based on making fuzzy the mappings $\pi: S \to \Sigma$, by having h act on wave-functionals of the form $\Psi [\pi(x); t]$. Then H is the sum of pairwise embedding or homotopy hamiltonians. The corresponding functional Schrodinger equation would simply describe the time evolution of quantised Skyrmions with the base space fixed and $\Sigma \in SU(2)$. There have been very few analyses of this class of problem and then the base space is usually taken to be E^3. We shall not give the explicit form of h as it is complicated, but wait to present the associated action.

In the absence of the QSD terms the time evolution in (26) can be formally written as a functional integral Equation 28:

$$\Psi\left[\{\pi\}; t'\right] = \int \prod_{\alpha \neq \beta} D\tilde{\pi}_{\alpha\beta} e^{iS[\{\tilde{\pi}\}]} \Psi\left[\{\pi\}; t\right] \tag{28}$$

where, using the continuum t limit notation, the action is a sum of pairwise actions Equation 29:

$$S\left[\{\tilde{\pi}\}\right] = \sum_{\alpha \neq \beta} S_{\alpha\beta}\left[\tilde{\pi}_{\alpha\beta}\right] \tag{29}$$

$$S_{\alpha\beta}\left[\tilde{\pi}\right] = \int_t^{t'} dt'' \int d^n x \sqrt{-g} \left[\begin{array}{l} \frac{1}{2} Tr\left(\partial_\mu \tilde{U}\tilde{U}^{-1}\partial^\mu \tilde{U}\tilde{U}^{-1}\right) \\ + \frac{1}{16} Tr\left[\partial_\mu \tilde{U}\tilde{U}^{-1}, \partial^\nu \tilde{U}\tilde{U}^{-1}\right]^2 \end{array}\right]$$

And the now time-dependent (indicated by the tilde symbol) mappings $\tilde{\pi}$ are parametrised by $\tilde{U}(x,t), \tilde{U} \in S_\alpha$. The metric $g_{\mu\nu}$ is that of the *n*-dimensional base space, S_β, in $\pi_{\alpha,\beta}: S_\beta \to S_\alpha$. As usual in the functional integral formalism the functional derivatives in the quantum hamiltonian, in (27), now manifest as the time components ∂_0 in the above equation, so now this has the form of a 'classical' action and we see the emergence of 'classical' fields, though the emergence of 'classical' behaviour is a more complex process. Equation 26 or (28) describe an infinite set of quantum skyrme systems,

coupled in a pairwise manner. Note that each homotopic mapping appears in both orders; namely $\pi_{\alpha\beta}$ and $\pi_{\beta\alpha}$.

Quantum State Diffusion

The Quantum State Diffusion (QSD) (Percival, 1998) terms are non-linear and stochastic Equation 30:

$$QSD = \sum_j \left(<L_j^\dagger> L_j - \frac{1}{2} L_j^\dagger L_j - <L_j^\dagger><L_j> \right) \Psi \Delta t$$
$$+ \sum_j \left(L_j - <L_j> \right) \Psi \Delta \xi_j \tag{30}$$

Which involves summation over the class of Linblad functional operators L_j. The QSD terms are up to 5th order in Ψ, as in general Equation 31:

$$<A>_t \equiv \int \prod_{\alpha \neq \beta} D\pi_{\alpha\beta} \Psi\left[\{\pi\};t\right] * A\Psi\left[\{\pi\};t\right] \tag{31}$$

And where $\Delta\xi_j$ are complex statistical variables with means $M(\Delta\xi_j) = 0$, $M(\Delta\xi_j\Delta\xi_{j'}) = 0$ and $M\left(\Delta\xi_j^*\Delta\xi_{j'}\right) = \delta(j - j')\Delta t$. The remarkable property of this QSD term is that the unitarity of the time evolution in (26) is maintained in the mean.

Emergent Classicality

These QSD terms are ultimately responsible for the emergence of classicality via an objectification (Percival 1998), but in particular they produce wave-function(al) collapses during quantum measurements, as the QSD terms tend to 'sharpen' the fuzzy homotopies towards classical or sharp homotopies. So the QSD terms, as residual SRN effects, lead to the Born quantum measurement random behaviour, but here arising from the Process Physics and not being invoked as a metarule. Keeping the QSD terms leads to a functional integral representation for a density matrix formalism in place of (28) and this amounts to a derivation of the decoherence formalism which is usually arrived at by invoking the Born measurement metarule. Here we see that decoherence arises from the limitations on self-referencing.

In the above we have a deterministic and unitary evolution, tracking and preserving topologically encoded information, together with the stochastic QSD terms, whose form protects that information during localisation events and which also ensures the full matching in QHFT of process-time to real time: An ordering of events, an intrinsic direction or 'arrow' of time and a modelling of the contingent present moment effect. So we see that Process Physics generates a complete theory of quantum measurements involving the nonlocal, non-linear and stochastic QSD terms. It does this because it

generates both the 'objectification' process associated with the classical apparatus and the actual process of (partial) wavefunctional collapse as the quantum modes interact with the measuring apparatus. Indeed many of the mysteries of quantum measurement are resolved when it is realised that it is the measuring apparatus itself that actively provokes the collapse and it does so because the QSD process is most active when the system deviates strongly from its dominant mode, namely the ongoing relaxation of the system to a 3D process-space and matter survives only because of its topological form. This collapse amounts to an ongoing sharpening of the homotopic mappings towards a 'classical' 3D configuration-resulting in essentially the process we have long recognised as 'space'. Being non-local the collapse process does not involve any propagation effects, that is the collapse does not require any effect to propagate through the space. For that reason the self-generation of space is in some sense action-at-a-distance and the emergence of such a quantum process underlying reality is, of course, contrary to the long-held belief by physicists that such action is unacceptable, though that belief arose before the quantum collapse was experimentally shown to display action at a distance in the Aspect experiment. Hence we begin to appreciate why the new theory of gravity does not involve the maximum speed c of propagation through space and why it does not predict the GR gravitational waves travelling at speed c, of the kind long searched for but not detected.

The mappings $\pi_{\alpha\beta}$ are related to group manifold parameter spaces with the group determined by the dynamical stability of the mappings. This symmetry leads to the flavour symmetry of the standard model of 'particle' physics. Quantum homotopic mappings or skyrmions behave as fermionic or bosonic modes for appropriate winding numbers; so Process Physics predicts both fermionic and bosonic quantum modes, but with these associated with topologically encoded information and not with objects or 'particles'.

Emergent Quantum Field Theory

The QHFT is a very complex 'book-keeping' system for the emergent properties of the neural network and we now sketch how we may extract a more familiar Quantum Field Theory (QFT) that relates to the standard model of 'particle' physics. An effective QFT should reproduce the emergence of the process-space part of the quantum foam, particularly its 3D aspects. The QSD processes play a key role in this as they tend to enhance classicality. Hence at an appropriate scale QHFT should approximate to a more conventional QFT, namely the emergence of a wave-functional system $\Psi[U(x); t]$ where the configuration space is that of homotopies from a 3-space to $U(x) \in G$, where G is some group manifold

space. This *G* describes 'flavour' degrees of freedom. So we are coarsegraining out the gebit structure of the quantum-foam. Hence the Schrodinger wavefunctional equation for this QFT will have the form Equation 32:

$$\Psi[U;t+\Delta t] = \Psi[U;t] - iH\Psi[U;t]\Delta t + QSD\,terms \qquad (32)$$

where, the general form of *H* is known and where a new residual manifestation of the SRN appears as the new QSD terms. This system describes skyrmions embedded in a continuum space. It is significant that such Skyrmions are only stable, at least in flat space and for static skyrmions, if that space is 3D. This tends to confirm the observation that 3D space is special for the neural network process system.

Emergent Flavour and Colour

Again, in the absence of the QSD terms, we may express (32) in terms of the functional integral Equation 33:

$$\Psi[U;t'] = \int D\tilde{U}e^{iS[\tilde{U}]}\Psi[U;t] \qquad (33)$$

To gain some insight into the phenomena present in (32) or (33), it is convenient to use the fact that functional integrals of this Skyrmionic form may be written in terms of Grassmann-variable functional integrals, but only by introducing a fictitious 'metacolour' degree of freedom and associated coloured fictitious vector bosons. This is essentially the reverse of the Functional Integral Calculus (FIC) hadronisation technique in the Global Colour Model (GCM) of QCD. The action for the Grassmann and vector boson part of the system is of the form (written for flat space) Equation 34:

$$S[\bar{p},p,A_\mu^\alpha] = \int d^4x \left(\begin{array}{c} \bar{p}\gamma^\mu\left(i\partial_\mu + g\frac{\lambda^a}{2}A_\mu^a\right)p - \\ \frac{1}{4}F_{\mu\nu}^a(A)F^{a\mu\nu}(A) \end{array} \right) \qquad (34)$$

where, the Grassmann variables $p_{fc}(x)$ and $\bar{p}_{fc}(x)$ have flavour and metacolour labels. The Skyrmions are then re-constructed, in this system, as topological solitons. These coloured and flavoured but fictitious fermionic fields $\bar{p}$ and p correspond to a preon system. As they are purely fictitious, in the sense that there are no excitations in the system corresponding to them, the metacolour degree of freedom must be hidden or confined. We thus arrive at the general feature of the standard model of particles with flavour and confined colour degrees of freedom. Then while the QHFT and the QFT represent an induced syntax for the semantic information, the preons may be considered as an induced 'alphabet' for

that syntax. The advantage of introducing this preon alphabet is that we can more easily determine the states of the system by using the more familiar language of fermions and bosons, rather than working with the skyrmionic system, so long as only colour singlet states are finally permitted. In order to establish fermionic behaviour a Wess-Zumino (WZ) process must be extracted from the iterator behaviour or the QHFT. Such a WZ process is time-dependent and so cannot arise from the frozen SRN. It is important to note that (34) and the action in (33) are certainly not the final forms. Further analysis will be required to fully extract the induced actions for the emergent QFT.

Hilbert Spaces

Process Physics has suggested the origin of quantum phenomena and of its Hilbert-space formalism. This phenomena is associated with the time evolution of the conserved topological defects embedded in the process space. However that embedding need not be local, as illustrated in Fig. 5. This particular situation corresponds to the Hilbert space 'sum':

$$\psi(x) = \psi_1(x) + \psi_2(x) \qquad (35)$$

where, $\psi_1(x)$ and $\psi_2(x)$ are non-zero only in the respective embedding regions. This is how quantum non-locality manifests in conventional quantum theory. So the Hilbert space 'sum' is the representation of the connectivity shown in Fig. 5. Such a non-local embedding is also responsible for the phenomenon of quantum entanglement.

Quantum Matter and Dynamical Space

The dynamics and detection of space is a phenomenon that physics missed from its beginning, with space modelled as a geometric entity without structure or time dependence. That has changed recently with the determination of the speed and direction of the solar system through the dynamical space and the characterisation of the flow turbulence: Gravitational waves. Detections used various techniques and have all produced the same speed and direction (Cahill 2005b; 2006a; 2006a; 2006b; 2006c; 2007; 2008; 2009a; 2009b; 2011; 2012; 2013a; 2013b; 2013d; 2014b; Cahill *et al*., 2000). The detected dynamical space was missing from all conventional theories in physics: Gravity, Electromagnetism, Atomic, Nuclear, Climate,... The detection of the dynamical space has led to a major new and extensively tested theory of reality.

Above we presented a "bottom up" theory. Here we present a "top down" theory that follows from a minimal extension of the quantum theory and the gravity theory by introducing the detected dynamical space.
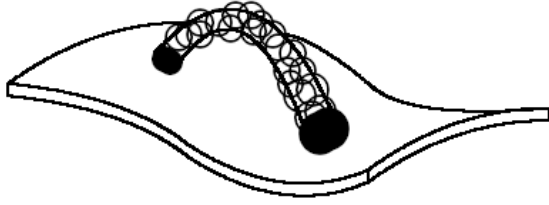
Fig. 5. The is a representation of the origin of quantum nonlocality. An entity is attached at two disjoint regions of the [3]-space with the gebit structure of that space not shown

The Schrodingier equation extension to include the dynamical space is, Cahill (2006c) Equation 36:

$$i\hbar\frac{\partial\psi(r,t)}{\partial t} = -\frac{\hbar^2}{2m}\nabla^2\psi(r,t) + V(r,t)\psi(r,t)$$
$$-i\hbar\left(v(r,t).\nabla + \frac{1}{2}\nabla.v(r,t)\right)\psi(r,t) \qquad (36)$$

Here $v(r, t)$ is the velocity field describing the dynamical space at a classical field level and the coordinates r give the relative location of (r, t) and $v(r, t)$, relative to a Euclidean embedding space and also used by an observer to locate structures. At sufficiently small distance scales that embedding and the velocity description is conjectured to be not possible, as then the dynamical space requires an indeterminate dimension embedding space, being possibly a quantum foam, as noted above. This minimal generalisation of the original Schrodingier equation arises from the replacement $\partial/\partial t \rightarrow \partial/\partial t + v.\nabla$, which ensures that the quantum system properties are determined by the dynamical space and not by the embedding coordinate system. The same replacement is also to be implemented in the original Maxwell equations, yielding that the speed of light is constant only wrt the local dynamical space, as observed and which results in lensing from stars and black holes. The extra $\nabla.v$ term in (36) is required to make the hamiltonian in (36) hermitian. Essentially the existence of the dynamical space in all theories has been missing. The dynamical theory of space itself is briefly reviewed below. The dynamical space velocity has been detected with numerous techniques, dating back to the 1st detection, the Michelson and Morley (1887), which was misunderstood and which lead to physics developing flawed theories of the various phenomena noted above. A particularly good technique used the NASA Doppler shifts from spacecraft Earth-flybys, Cahill (2009b), to determine the anisotropy of the speed of EM waves. All successful detection techniques have observed significant fluctuations in speed and direction: These are the actually "gravitational waves", because they are associated with gravitational and other effects. In particular we report here

the role of these waves in solar flare excitations and Earth climate science (Cahill, 2014b).

A significant effect follows from (36), namely the emergence of gravity as a quantum effect: A wave packet analysis shows that the acceleration of a wave packet, due to the space terms alone (when $V(r, t) = 0$), given by $g = d^2<r>/dt^2$, (Cahill, 2006c), gives Equation 37:

$$g(r,t) = \frac{\partial v}{\partial t} + (v.\nabla)v \qquad (37)$$

That derivation showed that the acceleration is independent of the mass m: whence we have the 1st derivation of the Weak Equivalence Principle, discovered experimentally by Galileo. As noted below the dynamical theory for $v(r, t)$ has explained numerous gravitational phenomena.

The experimental data reveals the existence of a dynamical space. It is a simple matter to arrive at the dynamical theory of space and the emergence of gravity as a quantum matter effect, as noted above. The key insight is to note that the emergent quantum-theoretic matter acceleration in (37), $\partial v = \partial t + (v.\nabla)v$, is also an independently, the constituent Euler acceleration $a(r, t)$ of the space flow velocity field Equation 38:

$$a(r,t) = \lim_{\Delta t \to 0}\frac{v(r + v(r,t)\Delta t, t + \Delta t) - v(r,t)}{\Delta t}$$
$$= \frac{\partial v}{\partial t} + (v.\Delta)v \qquad (38)$$

Which describes the acceleration of a constituent element of space by tracking its change in velocity. This means that space has a structure that permits its velocity to be defined and detected, which experimentally has been done. This then suggests, from (37) and (38), that the simplest dynamical equation for $v(r, t)$ is Equation 39:

$$\Delta.\left(\frac{\partial v}{\partial t} + (v.\nabla)v\right) = -4\pi G\rho(r,t); \nabla \times v = 0 \qquad (39)$$

Because it then gives $\nabla.g = -4\pi G\rho(r, t)$, $\nabla \times g = 0$, which is Newton's inverse square law of gravity in differential form.

Hence the fundamental insight is that Newton's gravitational acceleration field $g(r, t)$ for matter is really the acceleration field $a(r, t)$ of the structured dynamical space and that quantum matter acquires that acceleration because it is fundamentally a wave effect and the wave is refracted by the accelerations of space.

While the above leads to the simplest 3-space dynamical equation this derivation is not complete yet. One can add additional terms with the same order in speed spatial derivatives and which cannot be a priori neglected. There are two such terms, as in:

$$\Delta \cdot \left(\frac{\partial v}{\partial t} + (v.\nabla)v \right) + \frac{5\alpha}{4}\left((trD)^2 - tr\left(D^2\right) \right) + \dots = -4\pi G\rho$$

where $D_{ij} = \partial v_i = \partial x_j$. However to preserve the inverse square law external to a sphere of matter the two terms must have coefficients α and $-\alpha$, as shown. Here α is a dimensionless space self-interaction coupling constant, which experimental data reveals to be, approximately, the fine structure constant, $\alpha = e^2 / \hbar c$. The ellipsis denotes higher order derivative terms with dimensioned coupling constants, which come into play when the flow speed changes rapidly wrt distance. The observed dynamics of stars and gas clouds near the centre of the Milky Way galaxy has revealed the need for such a term (Cahill and Kerrigan, 2011) and we find that the space dynamics then requires an extra term:

$$\nabla \cdot \left(\frac{\partial v}{\partial t} + (v.\nabla)v \right) + \frac{5\alpha}{4}\left((trD)^2 - tr\left(D^2\right) \right)$$
$$+ \delta^2 \nabla^2 \left((trD)^2 \right) + \dots = -4\pi G\rho \tag{40}$$

where, δ has the dimensions of length and appears to be a very small Planck-like length. This then gives us the dynamical theory of 3-space. It can be thought of as arising via a derivative expansion from a deeper theory, such as a quantum foam theory, above. Note that the equation does not involve c, is non-linear and time-dependent and involves non-local direct interactions. Its success implies that the universe is more connected than previously thought. Even in the absence of matter there can be time-dependent flows of space.

Note that the dynamical space equation, apart from the short distance effect-the δ term, there is no scale factor and hence a scale free structure to space is to be expected, namely a fractal space. That dynamical equation has back hole and cosmic filament solutions (Cahill and Kerrigan, 2011; Rothall and Cahill, 2013), which are non-singular because of the effect of the δ term. At large distance scales it appears that a homogeneous space is dynamically unstable and undergoes dynamical breakdown of symmetry to form a spatial network of black holes and filaments, (Rothall and Cahill, 2013), to which matter is attracted and coalesces into gas clouds, stars and galaxies.

The dynamical space Equation 40 explains phenomena such as Earth bore-hole gravity anomalies, from which the value of α was extracted, flat rotation curves for spiral galaxies, galactic black holes and cosmic filaments, the universe growing/expanding at almost a constant rate, weak and strong gravitational lensing of light,.... A significant aspect of the space dynamics is that space is not conserved: It is continually growing, giving the observed universe expansion and is dissipated by matter. As well it has no energy density measure. Nevertheless it can generate energy into matter.

Detecting Dynamical Space Speed and Turbulence with Diodes

The Zener diode in reverse bias mode can easily and reliably measure the space speed fluctuations, Fig. 7 and two such detectors can measure the speed and direction of the space flow and waves, (Cahill, 2013d; 2014b). Consider plane waves with energy $E = \hbar\omega$. Then (36) with $v = 0$ and $V = 0$ gives $\psi = e^{-\omega t + ik \cdot r}$. When $v \neq 0$, but locally uniform wrt to the diode, the energy becomes $E \rightarrow E + \hbar k \cdot v$. This energy shift can be easily detected by the diode as the electron transmission current increases with increased energy. By using spatially separated diodes the speed and direction has been measured and agrees with other detection techniques.

Although this Zener diode effect was only discovered in 2013, (Cahill, 2013d), Zener diode detectors have been available commercially for much longer and are known as Random Event Generators, (REG). That terminology was based on the flawed assumption that the quantum tunnelling fluctuations were random wrt an average. However the data (Cahill, 2013d) showed that this is not the case. That experimental result contradicts the standard interpretation of "randomness" in quantum processes, which dates back to the Born interpretation in 1926. To the contrary the recent experiments show that the fluctuations are not random, but are directly determined by the fluctuations in the passing dynamical space.

The various detections of the dynamical space always showed turbulence/wave effects and we can represent the fractal structure of this space in Fig. 6.
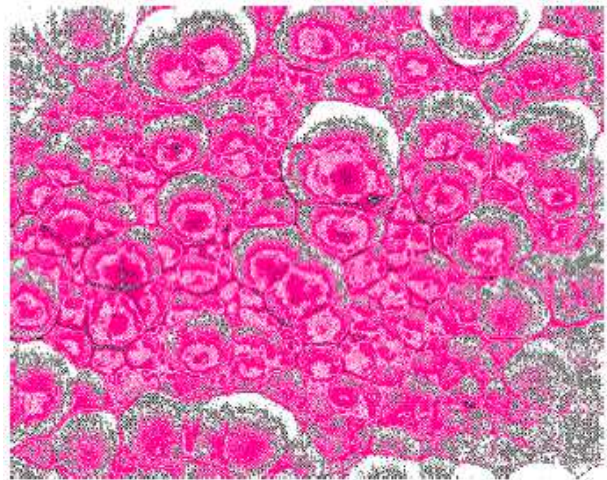

Fig. 6. Representation of the fractal wave data revealing the fractal textured structure of the 3-space, with cells of space having slightly different velocities and continually changing and moving wrt the Earth with a speed of ~500 km sec^{-1} and from a southerly direction This "pink space" is suggestive of the 1/f spectrum of the detected fluctuations
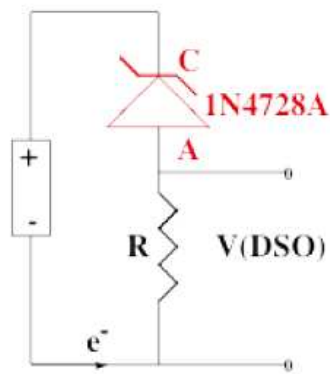
Fig. 7. Circuit of Zener Diode Gravitational Wave Detector, showing 1.5 V AA battery, 1N4728A Zener diode operating in reverse bias mode and having a Zener voltage of 3.3 V and resistor R = 10 KΩ. Voltage V across resistor is measured and used to determine the space driven fluctuating tunnelling current through the Zener diodes. Current fluctuations from two collocated detectors are shown to be the same, but when spatially separated there is a time delay effect, so the current fluctuations are caused by space speed fluctuations. Using diodes in parallel increases S/N

Neo-Lorentz Relativity

The major extant relativity theories-Galileo's Relativity (GaR), Lorentz's Relativity (LR) and Einstein's Special Relativity (SR), with the latter much celebrated, while the LR is essentially ignored. Indeed it is often incorrectly claimed that SR and LR are experimentally indistinguishable. It has been shown that (i) SR and LR are experimentally distinguishable, (ii) that comparison of gas-mode Michelson interferometer experiments with spacecraft earth-flyby Doppler shift data demonstrate that it is LR that is consistent with the data, while SR is in conflict with the data, (iii) SR is exactly derivable from GaR by means of a mere linear change of space and time coordinates that mixes the Galilean space and time coordinates (Cahill, 2013a). So it is GaR and SR that are equivalent. Hence the well-known SR relativistic effects are purely coordinate effects and cannot correspond to the observed relativistic effects. The connections between these three relativity theories has become apparent following the discovery that space is an observable dynamical textured system and that space and time are distinct phenomena, leading to a neo-Lorentz Relativity (nLR). The observed relativistic effects are dynamical consequences of nLR and 3-space. In particular in SR length contraction of rods and time dilation of clocks are supposedly caused only by motion wrt the observer, whereas in nLR these effects are caused by motion wrt the space local to the rods and clocks and apply only to actual rods and clocks. In

the case of Maxwell's EM theory the dynamical space is incorporated into the vacuum field equation by making the change $\partial/\partial t \rightarrow \partial/\partial t + v \cdot \nabla$ (Cahill 2009a).

Conclusion

The discovery that a dynamical space exists by Cahill and Kitto (2003) represented a dramatic turning point in our understanding of reality, since until then physicists had assumed that space and time, or even spacetime, were successful purely geometrical modellings of the phenomena of space and time and denied any notion that a dynamical 3-space exists which displays a flow velocity wrt an observer and which displays turbulence/gravitational wave effects. These are now easy to measure and characterise, exhibiting a fractal time dependent structure. This space is fundamental to all phenomena and we are now entering a new epoch in physics in which the role of space in all phenomena is now emerging, see for example the recent discoveries re solar flares and earth climate, (Cahill 2014b). Here we have reviewed two related aspects of this new physics: First we considered reality to be a self referencing stochastic network and showed that there is evidence that a dynamical fractal space arises and with quantum matter also arising as topological defects in the space. As well we have briefly discussed the consequences of modifying theories of the quantum, EM radiation and gravity by including a dynamical space modelled at the classical level by a velocity field. Of key significance is that in recent years a variety of new 3-space detection technologies have been devised, with the latest being the nanotechnology pn diode detection device, which is incredibly simple, cheap and robust. That success of that device demonstrated the standard interpretation of "quantum randomness" was incorrect, namely that the observed fluctuations were caused by the space passing through the diode.

Acknowledgment

Funding Information

Ethics

This article is original and contains unpublished material. The corresponding author confirms that all of the other authors have read and approved the manuscript and no ethical issues involved.

References

Cahill, R.T., 1989. Hadronisation of QCD. Aust. J. Phys., 42: 171-186. DOI: 10.1071/PH890171

Cahill, R.T., 1992. Hadronic laws from QCD. Nucl. Phys. A, 543: 63-78. DOI: 10.1016/0375-9474(92)90411-C

Cahill, R.T. and S.M. Gunner, 1998. The global colour model of QCD for hadronic processes: A review. Fizika B, 7 171-202.

Cahill, R.T. and C.M. Klinger, 2000. Self-referential noise and the synthesis of three-dimensional space. Gen. Rel. Grav., 32: 529-540. DOI: 10.1023/A:1001984518976

Cahill, R.T. and K. Kitto, 2003. Michelson-Morley experiments revisited and the cosmic background radiation preferred frame. Apeiron, 10: 104-117.

Cahill, R.T., C.M. Klinger and K. Kitto, 2000. Process physics: Modelling reality as self-organising information. Physicist, 37: 191-195.

Cahill, R.T., 2005a. Process Physics: From Information Theory to Quantum Space and Matter. 1st Edn., Nova Science Publishers, New York, ISBN-10: 1594543003, pp: 215.

Cahill, R.T., 2005b. The Michelson and Morley 1887 experiment and the discovery of absolute motion. Prog. Phys., 3: 25-29.

Cahill, R.T., 2006a. A new light-speed anisotropy experiment: Absolute motion and gravitational waves detected. Prog. Phys., 4: 73-92.

Cahill, R.T., 2006b. 3-Space in-flow theory of gravity: Boreholes, blackholes and the fine structure constant. Prog. Phys., 2: 9-16.

Cahill, R.T., 2006c. Dynamical fractal 3-space and the generalised Schrodinger Equation: Equivalence principle and vorticity effects. Prog. Phys., 1: 27-34.

Cahill, R.T., 2007. Optical-fiber gravitational wave detector: Dynamical 3-space turbulence detected. Prog. Phys., 4: 63-68.

Cahill, R.T., 2008. Unravelling lorentz covariance and the spacetime formalism. Prog. Phys., 4: 19-24.

Cahill, R.T., 2009a. Dynamical 3-Space: A Review. In: Ether Space-time and Cosmology: New Insights into a Key Physical Medium, Levy, J. and M.C. Duffy (Eds.), Apeiron, ISBN-10: 0973291184, pp: 135-200.

Cahill, R.T., 2009b. Combining NASA/JPL one-way optical-fiber light-speed data with spacecraft earth-flyby Doppler-shift data to characterise 3-space flow. Prog. Phys., 4: 50-64.

Cahill, R.T., 2011. Dynamical 3-Space: Cosmic filaments, sheets and voids. Prog. Phys., 2: 44-51.

Cahill, R.T. and D. Kerrigan, 2011. Dynamical space: Supermassive galactic black holes and cosmic filaments. Prog. Phys., 4: 79-82.

Cahill, R.T., 2012. Characterisation of low frequency gravitational waves from dual RF coaxial-cable detector: Fractal textured dynamical 3-space, Prog. Phys., 3: 3-10.

Cahill, R.T. and D. Rothall, 2012. Discovery of uniformly expanding universe. Prog. Phys., 1: 63-68.

Cahill, R.T., 2013a. Dynamical 3-space: Neo-lorentz relativity. Phys. Int., 4: 60-72. DOI: 10.3844/pisp.2013.60.72

Cahill, R.T., 2013b. Discovery of dynamical 3-space: Theory, experiments and observations-a review. Am. J. Space Sci., 1: 77-93. DOI: 10.3844/ajssp.2013.77.93

Cahill, R.T., 2013c. Nanotechnology quantum detectors for gravitational waves: Adelaide to London correlations observed. Prog. Phys., 4: 57-62.

Cahill, R.T., 2014a. Review of gravitational wave detections: Dynamical space. Phys. Int., 5: 49-86. DOI: 10.3844/pisp.2014.49.86

Cahill, R.T., 2014b. Solar flare five-day predictions from quantum detectors of dynamical space fractal flow turbulence: Gravitational wave diminution and earth climate cooling. Prog. Phys., 10: 236-242.

Coleman, S., J.B. Hartle, T. Piran and S. Weinberg, 1981. Quantum Cosmology and Baby Universes. 1st Edn., World Scientific Pub Co Inc., ISBN-10: 9810203454, pp: 300.

Kitto, K., 2002. Dynamical hierarchies in fundamental physics. Flinders University.

Manton, N.S. and P.J. Ruback, 1985. Skyrmions in flat space and curved space. Phys. Lett. B, 181: 137-140. DOI: 10.1016/0370-2693(86)91271-2

Manton, N.S., 1987. Geometry of skyrmions. Comm. Math. Phys., 111: 469-478. DOI: 10.1007/BF01238909

Michelson, A.A. and E.W. Morley, 1887. On the relative motion of the earth and the luminiferous ether. Am. J. Sci., 34: 333-345. DOI: 10.2475/ajs.s3-34.203.333

Nagels, G., 1985. Space as a "bucket of dust". Gen. Rel. Grav., 17: 545-557. DOI: 10.1007/BF00763048

Nicholis, G. and I. Prigogine, 1997. Self-Organization in Nonequilibrium Systems: From Dissipative Structures to Order Through Fluctuations. 1st Edn., J. Wiley and Sons, New York.

Ogden, R.W., 1984. Non-Linear Elastic Deformations. 1st Edn., Halstead Press, New York.

Parisi, G. and Y. Wu, 1981. Perturbation theory without gauge fixing. Scientia Sinica, 24: 483-496.

Percival, I., 1998. Quantum State Diffusion. 1st Edn., Cambridge University Press, Cambridge, ISBN-10: 0521620074, pp: 184.

Rothall, D.P. and R.T. Cahill, 2013. Dynamical 3-space: Black holes in an expanding universe. Prog. Phys., 4: 25-31.

Schrodinger, E., 1944. What is Life? The Physical Aspect of the Living Cell. 1st Edn., Cambridge University Press.